

The Time–Space Structure of the Asian–Pacific Summer Monsoon: A Fast Annual Cycle View*

LINHO

Department of Atmospheric Sciences, National Taiwan University, Taipei, Taiwan

BIN WANG

Department of Meteorology and the International Pacific Research Center, University of Hawaii at Manoa, Honolulu, Hawaii

(Manuscript received 25 April 2001, in final form 4 December 2001)

ABSTRACT

Despite the seemingly intricate and multifold time–space structure of the mean Asian–Pacific summer monsoon (APSM), its complexity can be greatly reduced once the significance of *fast annual cycles* has been recognized and put into perspective. The APSM climatology is characterized by a slowly evolving seasonal transition (*slow annual cycle*) superposed by pronounced singularities in the intraseasonal timescale, termed the “fast annual cycle” in this study. The fast annual cycles show nonrepetitive features from one episode to another, which are often divided by abrupt change events. The APSM fast annual cycles are composed mainly of two monsoon outbreaks, each marking a distinctive dry–wet cycle. The first cycle spans from the middle of May to early July and the second cycle from late July to early September. When the first cycle reaches its peak in mid-June, a slingshot-like convection zone, described as the grand-onset pattern, rules an area from the Arabian Sea to the Indochina Peninsula then bifurcates into a mei-yu branch and a tropical rain belt in the lower western North Pacific. After a brief recess during 20–29 July, the APSM harbors another rain surge in mid-August. This time a giant oceanic cyclone intensifies over the western North Pacific (around 20°N, 140°E); thus the rainy regime jumps 10°–15° north of the previous rain belt. This ocean monsoon gyre incubates numerous tropical cyclones. Meanwhile, the convection zone of the Indian monsoon intensifies and extends well into the subcontinent interior.

From the first to second cycle the major convection center has shifted from the adjacent seas in the northern Indian Ocean to the open ocean east of the Philippine Islands. The major cloud movement also switches from a northeastward direction in the Indian Ocean to a northwestward direction over the western North Pacific.

The two monsoon cycles turn out to be a global phenomenon. This can be shown by the coherent seasonal migration of upper-level subtropical ridgelines in the Northern Hemisphere. During the first cycle all the ridgelines migrate northward rapidly, a sign that the major circulation systems of boreal summer go through a developing stage. After 20–29 July, they reach a quasi steady state, a state in which all ridgelines stand still near their northern rim throughout the entire second cycle.

A reconstructed fast annual cycle based on four leading empirical orthogonal function modes is capable of reproducing most fine details of the APSM climatology, suggesting that the subseasonal changes of the mean APSM possess a limited number of degrees of freedom. A monsoon calendar designed on the basis of fast annual cycles (FACs) gives a concise description of the APSM climatology and provides benchmarks for validating climate model simulations.

1. Introduction

It is a common practice to take the first three or four harmonics of yearly time series as the annual cycle, which represents the smooth seasonal transition, a connotation of the seasonal solar forcing [hereafter, we refer this component as the *slow annual cycle* (SAC)]. Yet

in many places on earth the mean annual variation cannot in any realistic way be described as a slow annual cycle. Many rapidly changing events tend to be phase locked in time and space, resulting in a subseasonal component superposed on the slow annual cycle. A well-known example is the onset of the Indian summer monsoon, the local rainy season arriving in the beginning of June each year in which the standard deviation of onset dates in South Kerala was found to be less than nine days (Ananthakrishnan and Soman 1988). The snow accumulation and ablation provide another example. Observations from space (Leathers and Robinson 1997) showed that in North America the rapid snow accumulation and ablation tend to concentrate only

* International Pacific Research Center Contribution Number 163 and School of Ocean and Earth Science Contribution Number 6007.

Corresponding author address: Dr. LinHo, Department of Atmospheric Sciences, National Taiwan University, Taipei, Taiwan.
E-mail: linho@linhol.as.ntu.edu.tw

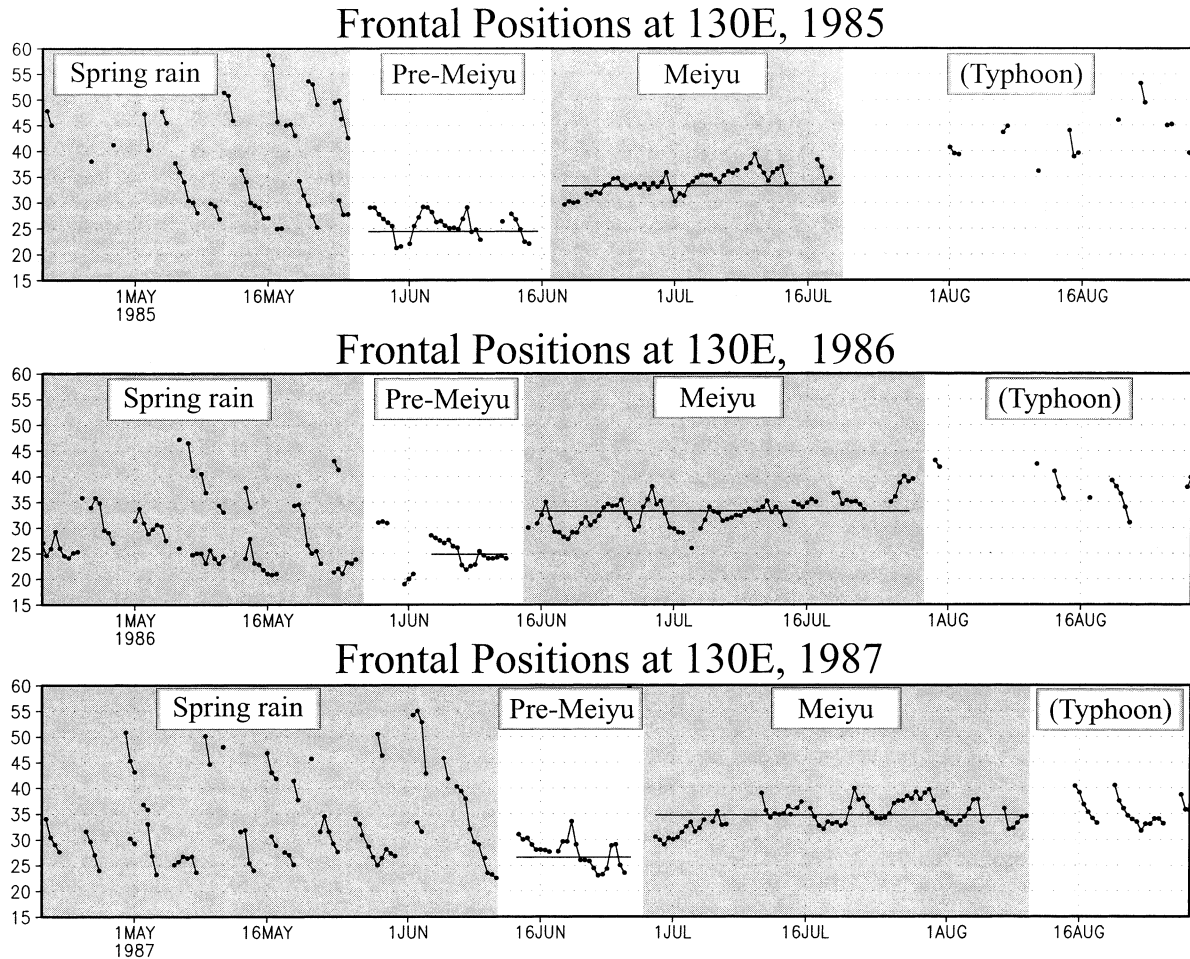


FIG. 1. The trajectories of cold fronts intersecting longitude 130°E. The subseasonal modulation of fronts appears distinctive. In spring the cold fronts move fast and migrate from north to south. The brief pre-mei-yu period marks the stationary front around 25°N, then it jumps to 35°N in the mei-yu position. Note that the changes are abrupt and phase-locked with the calendar. After the end of Jul, East Asia is mainly in the typhoon period.

within a certain calendar week. The ends of October and November signal two peaks in which snow amasses. Several teleconnection patterns are also known to bur-nish at a particular time on the calendar. For instance, a Rossby wave train was found emanating from the western North Pacific to North America (Ueda et al. 1995) just around the 42d Julian pentad (~25 July). This teleconnection pattern has sharp definition in time and space even to be extracted from a climatological time series.

Indeed, a rich variety of weather events occurs reg-ularly at a particular time and place. Lanzante (1983) coined those spikes and spears in climatological annual cycle the *singularities*. The Asian-Pacific summer mon-soon (APSM) system, sensitive to seasonal change, is particularly renowned for its abundance of singularities. A case at hand is shown in Fig. 1, which marks the positions of the front intersecting the longitude 130°E from 1985 to 1987. It is clear that the speed, direction,

and location of fronts are dictated by certain intrasea-sonal modulation, each envelope lasting about several weeks and highly phase locked to the calendar. All those monsoon subseasons are familiar to local people since they occur regularly every year.

A substantial part of those monsoon singularities is closely related to the tropical intraseasonal oscillations, as Kang et al. (1989) and Wang and Xu (1997) readily indicated. Many monsoon events are just manifestations of extreme phases of phase-locked summer intrasea-sonal oscillation. Nakazawa (1992) showed that two prominent climatological surges of low-level westerlies, derived from a 10-yr dataset, trigger several important abrupt change events, including the withdrawal of Baiu. Normally, the east Asian summer monsoon would go through four or five stages of stepwise seasonal tran-sition (Ding 1994). The division of subseasons and the issue of abrupt changes have been studied extensively within the monsoon community for many years (e.g.,

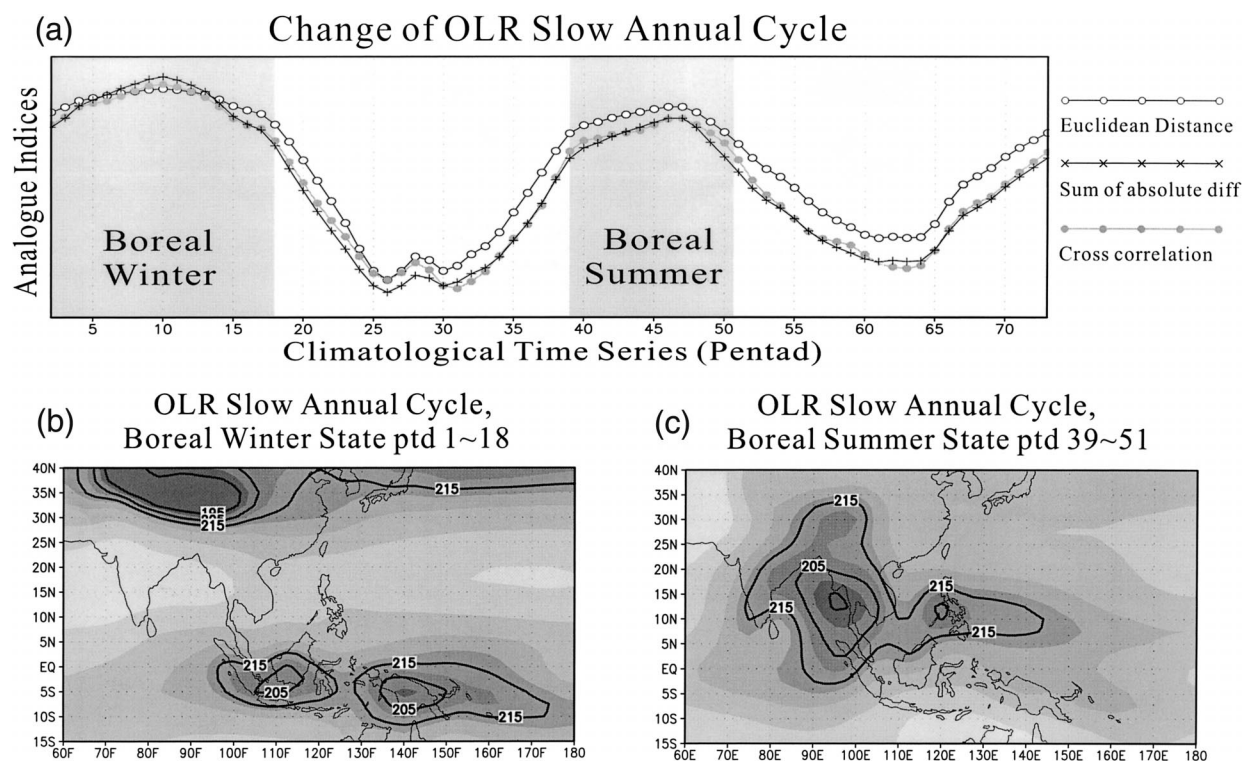


FIG. 2. The OLR SAC changes rather slowly from (b) the boreal winter state to (c) the boreal summer state. The changes of maps between two neighboring pentads are measured by the analog indices, in which a high value indicates very little change between two neighboring pentads. The analog indices are the Euclidean distance, sum of the absolute difference, and cross correlation between two maps. At pentad 26 the SAC experiences the most intense change from winter to summer. In (b) and (c) the boreal summer and winter states are very similar to a standard Jun–Jul–Aug (JJA) and Dec–Jan–Feb (DJF) average. The contour lines are in units of $W m^{-2}$.

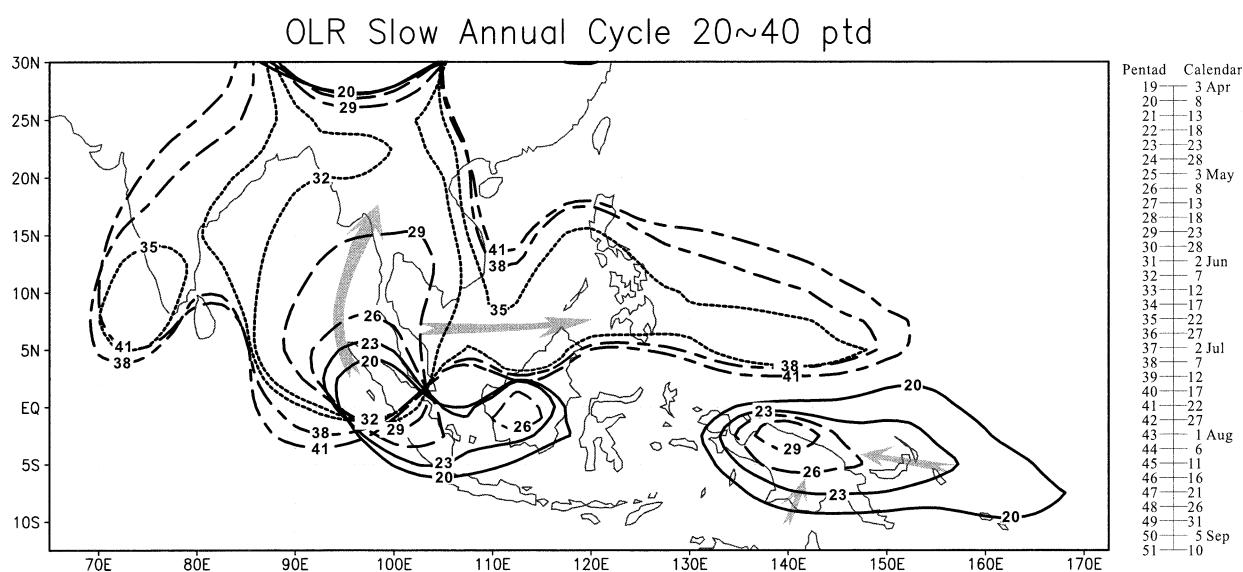


FIG. 3. The evolution of the OLR APSM slow annual cycle from pentad 20 to 40. The contours represent isolines where $OLR = 220 W m^{-2}$ and are labelled by pentad. The northward advancing of SAC deep convection from west of Sumatra toward the Bay of Bengal during pentad 23–29 marks the earliest rain surge for the APSM. It is coincident with the diminishing of convection over New Guinea around pentad 23. The SAC convection dominates the summer monsoon yet it changes very little after mid-Jun.

(a) The APSM First Fast Annual Cycle --- OLR

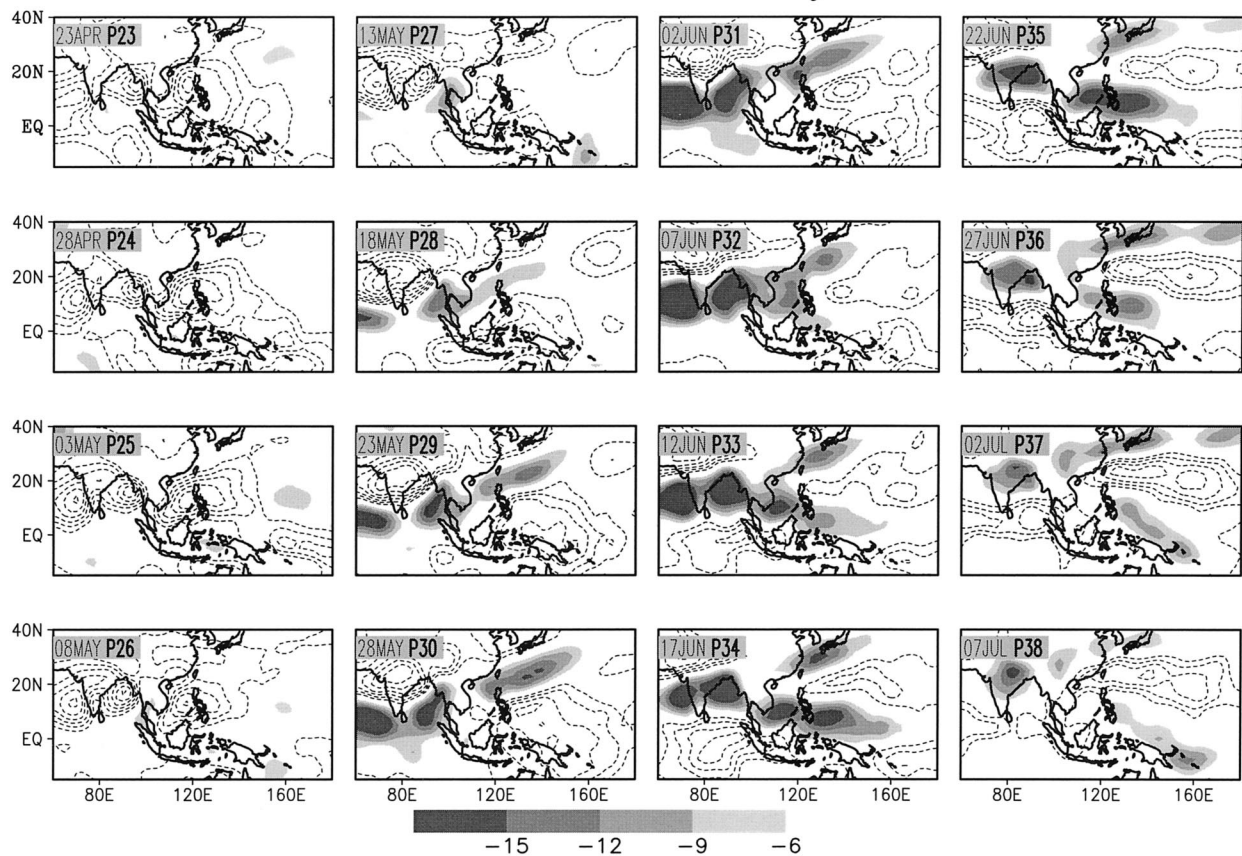


FIG. 4. A chronicle of fast annual cycle extracted from the pentad mean OLR for the Asian-Pacific summer monsoon. The shaded area indicates heavy rain and the dashed-line area marks the dry zone. The fast annual cycle maps show a continuation in time and 2D domain: (a) the first FAC that reaches peak phase, the grand-onset event at pentad 33–34; (b) the second FAC where the monsoon gyre intensifies from pentad 42 to 46.

Yoshino 1965; Kato 1985; Ninomiya and Muraki 1986; He et al. 1987; Tao and Chen 1987; Lau et al. 1988; Matsumoto 1992; Kawamura and Murakami 1998, etc.)

Wang and Xu (1997) proposed to name those intraseasonal components of climatological time series the *climatological intraseasonal oscillations* (CISO). They were able to identify four subseasonal cycles of the APSM, which were tested rigorously for statistical significance. Wang and Xu's results revealed that each CISO event has a coherent dynamical structure and propagates in a systematic way, thus nearly qualifying as a physical mode on climatological maps. Kang et al. (1999) continued the effort to extract from the APSM climatology a few important intraseasonal oscillation modes. Those modes were deduced from the EOF analysis of high cloud data of the International Satellite Cloud Climatology Project (ISCCP). This type of data appears quite adaptable to highlighting extratropical stationary fronts. Therefore, their results revealed more of CISO's characteristics north of 30°N in east Asia. Along the same track, Wu and Wang (2000) studied the multistage onset of the summer

rainy season in the western North Pacific, an area displaying distinctive abrupt changes and subseasons during the boreal summer.

Whereas the idea of the CISO emphasizes the phase-locking feature of the transient intraseasonal oscillation to the annual cycle, many varieties composing the monsoon singularities will not be limited and should not be all attributed to oscillating behavior (in the same context, e.g., as the wintertime Madden-Julian oscillations). In light of the fact that the large-scale summer monsoon circulation undergoes fundamental changes within a few weeks, and most subseasonal episodes will not repeat themselves in any periodic manner (except perhaps those from the tropical Indian Ocean northward and those from the tropical Pacific in a northwest direction), a new term, "*fast annual cycle*" (FAC) is proposed here to embrace more varieties of the APSM singularities and to restore the chronological order of events. Under this new term we will stress the parallel between the slow and fast annual cycles and focus on the synoptic climatology aspects. While both the FAC and CISO share the same deduction process (and the same level

(b) The APSM Second Fast Annual cycle --- OLR

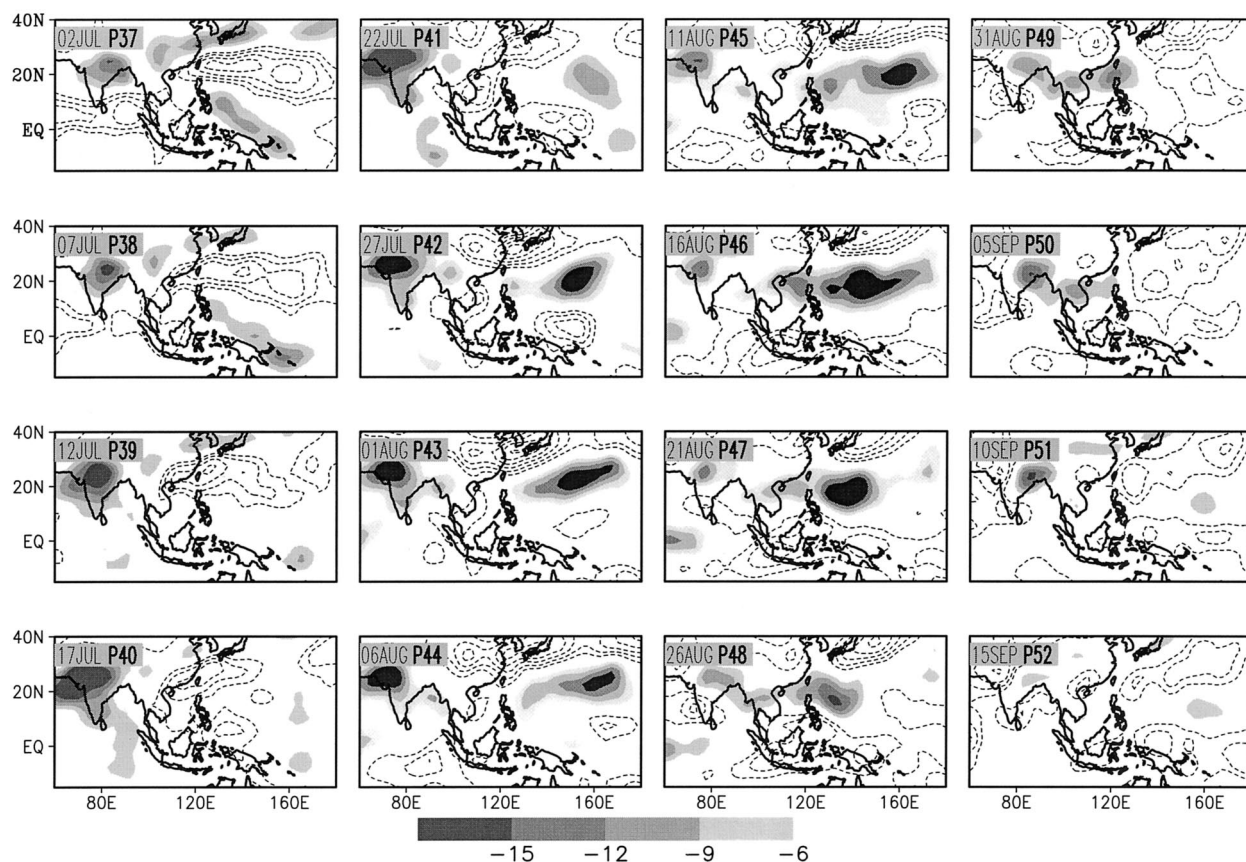


FIG. 4. (Continued)

of statistical significance), the term CISO can be saved for situations where the characteristics of tropical intraseasonal oscillation appear most evident.

It is the purpose of this study to construct the APSM climatological time-space structure in one continuum based on the slow and fast annual cycles. Section 2 describes data type and analysis procedure. Section 3 discusses the slow annual cycle, an essential element to lay the background for more rapid development of the fast annual cycle. Section 4 documents the fast annual cycles in pentad resolution. By treating a domain of $10^{\circ}\sim 30^{\circ}\text{N}$, $60^{\circ}\sim 180^{\circ}\text{E}$, it was found that the boreal summer can be divided into two grand cycles, each highlighting a major monsoon outbreak centered in the Indian and Western North Pacific (WNP) regions. The relative importance of these two monsoon outbreaks appears never been fully recognized and put into one time-space continuum. Section 5 pins down two major monsoon outbreaks. We postulate that the timing and pattern of these two major monsoon outbreaks are the backbone of the APSM evolution, as can be seen in the fact that the bulk rain movement changes drastically between two cycles. Evidence is also provided in section 6 that the two APSM FACs are part of a global-scale phenomenon.

Plotting the upper ridgelines reveals that the first cycle delineates a transient stage. The boreal summer circulation reaches a mature state only during the second cycle. An empirical orthogonal analysis in section 7, recapturing most of the APSM climatological features, suggests that the fast annual cycles in the mean APSM can be treated by a dynamical system with very limited degrees of freedom. In the last section, we deliver a monsoon calendar summing up both the SAC and FAC and recommend using FAC as a benchmark for numerical simulation of the APSM.

2. Data and methods

The majority of our datasets have pentad or finer resolution, aligned over the period from 1979 to 1999. They consist of 1) the outgoing longwave radiation (OLR) data from National Oceanic and Atmospheric Administration (NOAA) satellites; 2) the Climate Prediction Center's (CPC) data, merged analysis of precipitation (CMAP) data (Xie and Arkin 1997), which is produced by merging raingauge data, five kinds of satellite estimates [Geostationary Operational Environmental Satellite (GOES) Precipitation Index (GPI),

OLR-based precipitation index (OPI), special sensor microwave/imager (SSM/I) emission and Microwave Sounding Unit (MSU)], and numerical model predictions; 3) the National Center for Environmental Prediction–National Center for Atmospheric Research reanalysis data [hereafter referred to as the NCEP reanalysis data; Kalnay et al. (1996)], a dataset generated from a “frozen” version of the NCEP medium-range forecast model and operational spectral statistics interpolation procedure; 4) the typhoon track records, a set of daily track positions supplied by the Joint Typhoon Warning Center (JTWC); and 5) the twice-daily weather maps published by the Japan Meteorological Agency. The first three datasets have a space resolution of $2.5^\circ \times 2.5^\circ$.

The climatological annual cycle time series at each grid was decomposed into slow and fast annual cycle components. The filter used in this study was originally designed by Tanaka (1992) with only minor modification. The SAC was obtained by first using a 1–2–1 filter to remove weather noise, then applying a 19-pentad running-box mean over the climatological time series. It leads to the removal of 95% of fluctuations with periods less than 60 days. After subtracting the slow annual cycle, the resultant time series with periods ranging from 7.5 to 60 days is defined as the FAC.

3. The slow annual cycle in the APSM

The slow annual cycle in the APSM represents almost the June–July–August (JJA) averaged rainfall state. In seasonal transition the SAC accounts for the important northward advance of rain belt from the west of Sumatra to Myanmar around late March. Yet the SAC changes so sluggishly in pentad sequence, to grasp its transformation we applied a variety of analog indices, which measure the resemblance between two maps in neighboring pentads.

Figure 2a shows the yearly time series of three analog indices: the Euclidean distance, the sum of the absolute differences, and cross correlation between two sequential maps (available in the CDIST/DCDIST program, Hierarchical Cluster Analysis, the IMSL Math Library), of the outgoing longwave radiation (OLR) SAC over the APSM domain $15^\circ\text{S}\sim 40^\circ\text{N}$, $60^\circ\sim 180^\circ\text{E}$. Figure 2a has been arranged so that the ordinate points upward to indicate less change between two pentads. It can be seen that all three analog indices show similar results, that the SAC oscillates between two equilibrium states. The boreal winter state lasts from pentad 1 to 18 (Jan to late Mar, Fig. 2b) and the boreal summer state from pentad 39 to 51 (middle of Jul to mid Sep, Fig. 2c). During these two periods, the OLR pattern remains almost unchanged. Between these two states the SAC goes through the transitional stages.

The SAC varies relatively hastily around pentad 26 (early May), while the starting time for SAC seasonal transition can be traced back to as early as late March.

It signals that strong convection west of Sumatra begins to migrate north toward the Andaman Sea, as shown in Fig. 3. During the same period a patch of westerly wind emerges in the tropical Indian Ocean, near the tip of the Indian Peninsula. This wind patch soon manifests itself as part of giant wind gyre over the tropical Indian Ocean. The timing of this event appears dictated by the interaction between the seasonal insolation and land–sea contrast surrounding the northern Indian Ocean. The rapid growth of the cloud cluster and the subsequent northward movement of convection in the Bay of Bengal thrive from pentad 26 to 29 (Fig. 3), a development closely related to the development of a near-surface heat low over the Indian Peninsula (figure not shown). Soon after, the strong southeasterly over the Bay of Bengal brings convection to the Andaman Sea, and Myanmar and Thailand, who experience the earliest rainy season of the boreal summer monsoon.

At pentad 28 the new diabatic-heating center is established over the western Indochina Peninsula. As the southwestern flow surges to the southern South China Sea, it forces a series of downstream adjustments in the form of the FACs, including the withdrawal of the western Pacific subtropical high ridge and the onset event of the South China Sea. The establishment of the Bay of Bengal convection is also felt in the west, where the intensification of wind gyre in the tropical Indian Ocean, and the development of upper-level South Asia high, sends another surge of southwesterlies, setting the stage for a major monsoon outbreak on 10 June, as shown later. The SAC reflects the large-scale seasonal transition of continent and ocean that forces more rapid changes of the fast annual cycles.

4. The fast annual cycles in the APSM

In this section we document the fast annual cycles using the OLR pentad time series. The time series is divided into two cycles, each containing a major monsoon outbreak. Figures 4a,b sketch the climatological OLR time series filtered by the FAC frequency window. Figure 5 is a pseudoschematic diagram based on real data but vital parts have been enhanced. This diagram illustrates the lower circulation conditions during two FACs, where the East Asia monsoon, particularly the western Pacific subtropical high, is highlighted.

a. The first APSM FAC

Before mid-May the rain pattern is dominated by the slow annual cycle (Fig. 3). There are little traces of the fast annual cycle mode in sight (see Fig. 4a, from late Apr to mid-May). The western Pacific subtropical high ridge extends deeply into Indochina via the northern South China Sea, as shown in Fig. 5a. A critical time falls at pentad 28 (16–20 May). At this particular pentad, the APSM shows precursory signs for a major outbreak. It starts one pentad after the western ridge of the

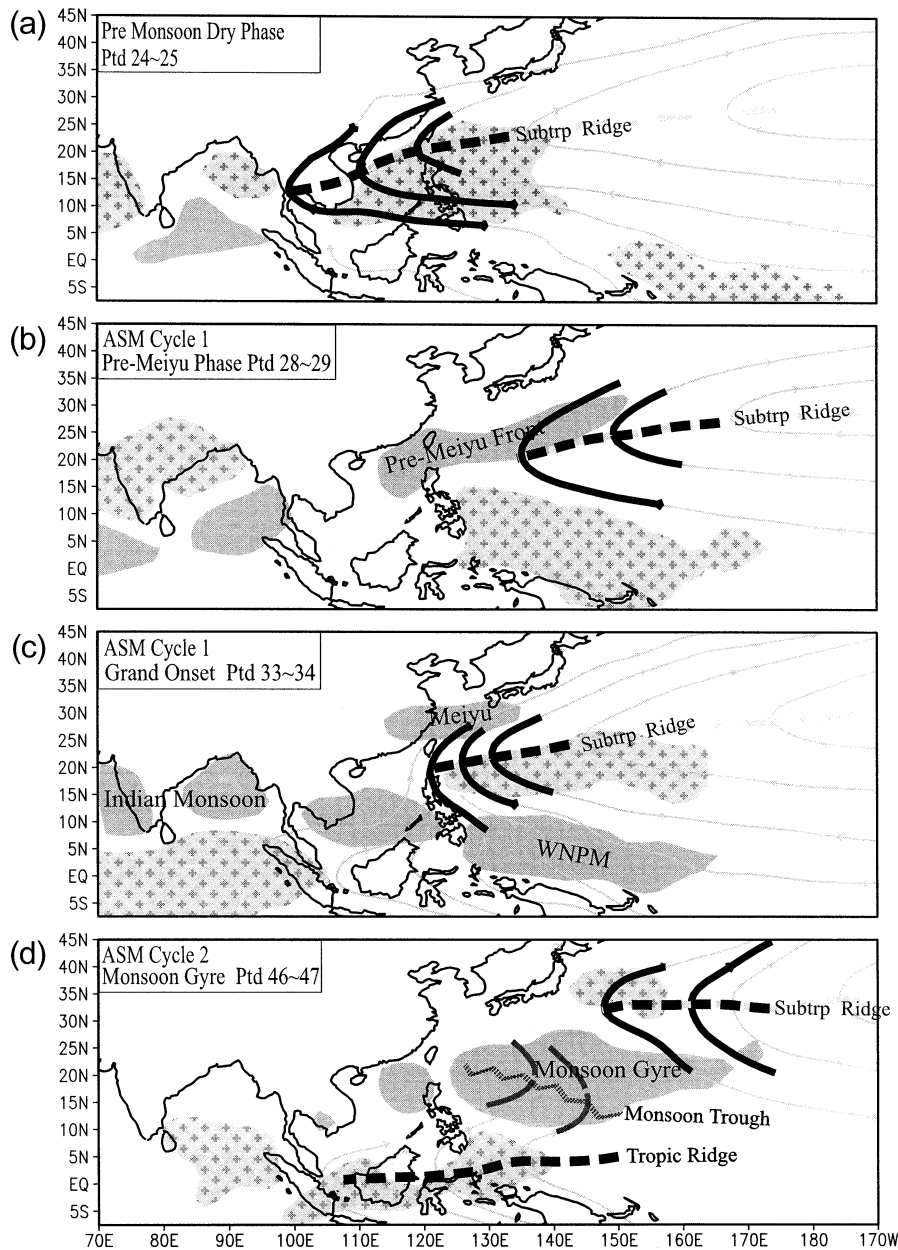


FIG. 5. A pseudoschematic diagram based on real data, illustrating a four-stage evolution [(a)–(d)] of the APSM. The emphases are on the East Asia side and the linkage between the western Pacific subtropical high ridge and monsoon rain. The shaded areas represent the rain patches and the cross-shaded areas mark the dry zones. The 850-hPa flow pattern has been enhanced.

western Pacific subtropical high has retreated suddenly toward the northeast, leaving the South China Sea a void for convection invasion, as shown in Fig. 5b. For the first time of the year the monsoon-scale southwestern flow is able to penetrate into the South China Sea and induces a lasting rainy season there. A convection zone in the form of stationary front (pre-mei-yu front) quickly establishes its position along the northern flank of the western Pacific subtropical high at pentad 29. The west-

ern Pacific subtropical high now retreats but intensifies. This establishment of stationary front manifests so that the low-level southwestern flow from the Indochina Peninsula finally manages to interact with the subtropical weather systems roving along the East Asian coast since spring. Boosted by the warm and moist low-level southwesterly, the front embeds many mesoscale convection cells (Chen and Chang 1980), which brings a short rainy season to Taiwan and the Okinawa area. This

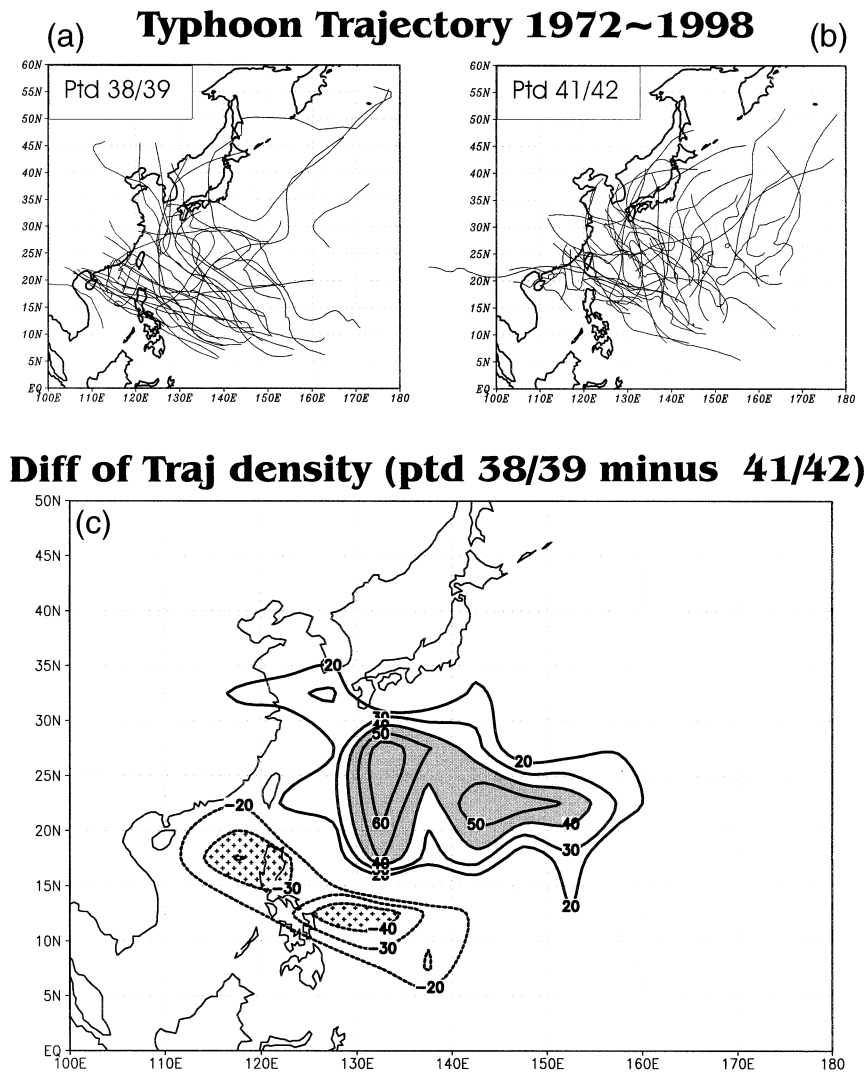


FIG. 6. The 27-yr typhoon tracks that fall into pentads (a) 38–39 and (b) 41–42, respectively. To subtract typhoon occurrences (a) from (b), (c) manifests the climatological difference of typhoon tracks between two bipentads. It can be seen that the jump of typhoon tracks fits perfectly the change of western North Pacific monsoon domain between the first and second FAC in Fig. 5. Thus the modulation of typhoon occurrences is also dictated by the phase-locked fast annual cycles.

short rainy season is called the pre-mei-yu (preflood or presummer, Fig. 5b) period by some studies (e.g., Ding 1994).

The pre-mei-yu period, a very localized rain spell confined to southeastern Asia in May, was also recognized by He et al. (1987) and Yanai et al. (1992). They called this rainy season the first transition period in contrast to the second transition period, which features the Indian monsoon onset. In Fig. 5b a four-cell structure largely dominates this mid-May pattern. The pre-mei-yu front tends to be short and easily overlooked also by fact that in 15% of years the pre-mei-yu period was delayed, hence making it indistinguishable from the mei-yu period (Lu and Chen 2001). For those “empty

mei-yu” (Taiwan mei-yu) years East Asia appears to plunge into the grand-onset pattern without much trace of a pre-mei-yu front. Thus, the absence, rather than the presence, of the pre-mei-yu front deems it obscure. Nevertheless, it is an essential local rainy feature in East Asia, as evident in Fig. 1.

Almost simultaneously the Indian monsoon rainfall bursts forth in the southern Arabian Sea. The precursory time also falls at pentad 28. From there, another super cloud cluster in the tropical Indian Ocean prospers on its way to the western coast of the Indian Peninsula and grows in sync with the convection over the Bay of Bengal. In the next six pentads (late May to late June; see relevant boxes in Fig. 4a) the monsoon trough intensifies

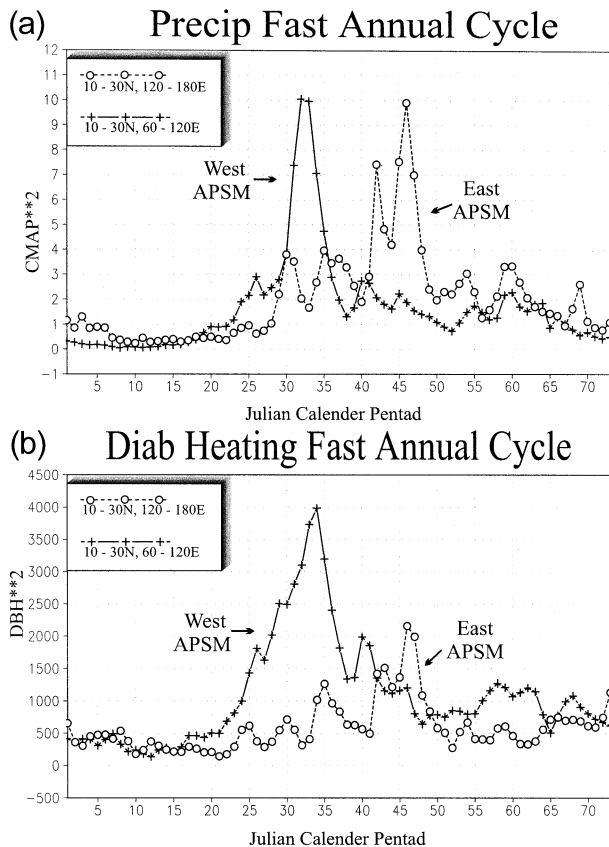


FIG. 7. (a) The square of the CMAP FAC and (b) the square of the vertically integrated diabatic heating FAC derived from the NCEP–NCAR reanalysis data. The cross-thin line denotes the value averaged over the west domain (10° – 30° N, 60° – 120° E) of the APSM, a region including the Arabian Sea, Indian Peninsula, and Bay of Bengal. The dot-dashed line is averaged over the east domain (10° – 30° N, 120° – 180° E), which covers coastal China and the western North Pacific. The two prominent monsoon outbreaks are seen in both fields.

at the Bay of Bengal and the Arabian Sea. The short pre-mei-yu rainy season suffers a mild recession at pentad 32. This break can also be recognized vividly from the frontal position map in Fig. 1, where the short, stationary front around 25° N holds its position until mid-June, then jumps to 32° – 35° N to signal the coming of mei-yu onset.

On the west of the Indochina Peninsula the FAC convection develops later than the pre-mei-yu period. Nevertheless the Indian monsoon has a strength dominating the first cycle since it extracts energy from a larger and more compact monsoon circulation (Krishnamurti and Bhalme 1976). From late May to late June, the strong convection over the Arabian Sea and the Bay of Bengal has advanced from the Tropics to reach the northern rim of the Indian Ocean (see Fig. 4a, pentads 28–31). Once the convection has filled up the adjacent seas on both sides of the Indian Peninsula, it starts to extend eastward (Fig. 4a, pentad 32–35). This time (Fig. 4a, pentad 32, 5–9 June), the east component of the monsoon trough

bifurcates from Indochina into a fork-shape rainy zone. The northern branch is the mei-yu stationary front and the southern branch aligns a series of disturbances along the southern South China Sea and the lower western North Pacific. Figure 5c reveals that the bifurcation is induced by strong wedging of the intensified western Pacific subtropical high. Its northern flank lines up the mei-yu front on the lower reach of the Yangtze River. On the southern flank the rain from the southern South China Sea keeps spreading along the island arc until it thins down near equatorial New Guinea (5° N, 150° E). By pentad 33 (11–15 June), the lower western North Pacific experiences its first rain spell and the Indian monsoon and mei-yu are simultaneously established. Figure 5c illustrates that an East Asia band structure comprises the mei-yu/subtropical ridge/western North Pacific monsoon. This episode is consistent with the extended EOF analysis of the summer intraseasonal oscillation by Lau and Chan (1986, their Fig. 7), only here the picture fits more precisely to a Julian calendar.

The peak phase of this cycle arrives at pentad 34 (Fig. 4a, 15–20 June). A continental-size fork-shape convection zone emerges that dominates the APSM region. Described as the “grand-onset” pattern by Wang and Xu (1997), it manifests a disturbance of global scale (Webster 1996). The grand-onset pattern exhibits four strong convection foci, three of them located at the semienclined seas, that is, the Arabian Sea, the Bay of Bengal, and the South China Sea, and the fourth one, being a hatchery for tropical storms, over the lower western North Pacific (also see the EOF mode 2 in section 7). There is a relatively weak northern branch, the mei-yu front, composed of the rainmaking elements from the midlatitude. The subsidence patches are fittingly tucked in the tropical Indian Ocean and in a shield region over the subtropical Pacific ($\sim 20^{\circ}$ N). In all, the convection zone is found to be divided into three parts; the Indian monsoon, the East Asian monsoon (mei-yu/baiu) and the western North Pacific monsoon. These three components will soon split after pentads 33 and 34 and drift apart. After pentad 38 there is hardly any trace of FAC-related convection over the APSM region; only the SAC convection is left. The APSM FAC goes into a remission that brings fair weather for most of the APSM in mid-July.

b. The second APSM FAC

Figure 4b depicts the evolution of the second APSM FAC. From pentad 37 to 41 (July, except the last week) the subtropical high occupies the western Pacific between 15° and 30° N. East Asia experiences a relatively dry spell except for the weak mei-yu still migrating toward northern China and Korea. During this recession a weakening of easterly winds around 20° N induces rapid warming of SST east of the Luzon Strait. Ueda and Yasunari (1996) suggested that the diminishing of wind stress is related to propagation of a teleconnection pattern emitted from the previous western North Pacific

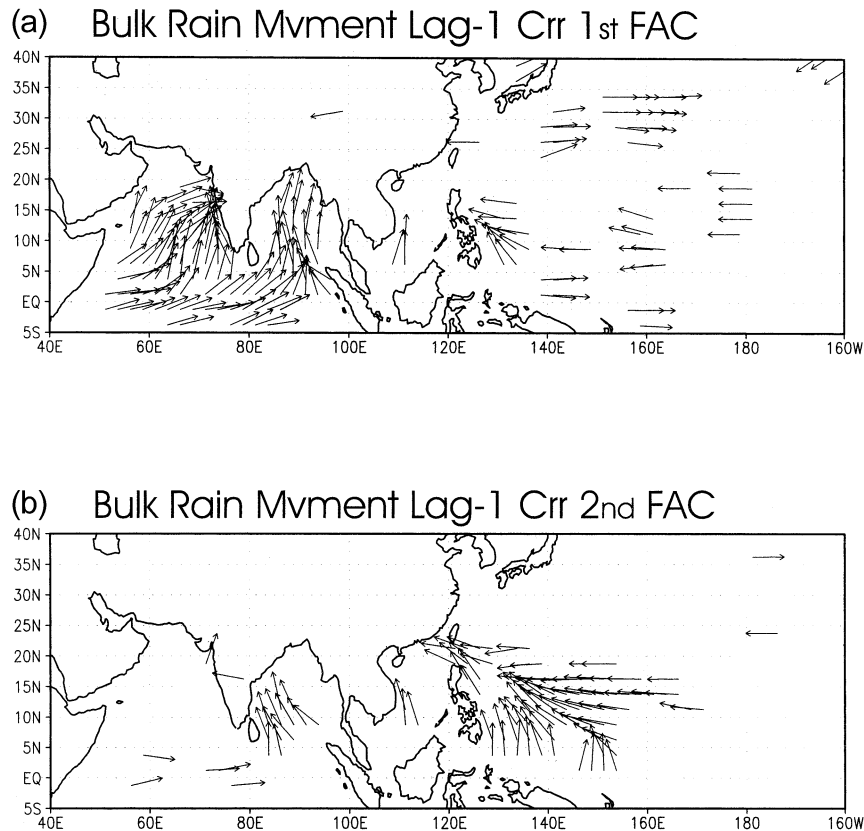


FIG. 8. The direction of bulk rain movement associated with (a) the first and (b) the second fast annual cycle. The arrows point to the position that shows the maximum value of (one pentad) lag correlation. Arrow length is proportional to the magnitude of lag correlation.

heating, which can be identified as the convection over the lower western North Pacific during the first FAC. Therefore, the first rainy season in the lower western North Pacific leads to the warming of SST farther north. Twenty days later, the warm SST triggers the second rainy season in the upper western North Pacific. This scenario is consistent with observations by Wu and Wang (2000).

The warm SST over the western North Pacific appears to coincide with the deepening of the tropical upper-troposphere trough (Sadler 1976; Chen and Yen 1991) at the same time, to compose a favorable environment for tropical disturbances. These factors can now generate a giant oceanic cyclone. At pentad 41 (see Fig. 4b, 20–24 July) convection explodes suddenly over the open ocean around 20°N, 160°E. It quickly leads to the formation of a strong low-level cyclonic circulation at 25°N. An eastward trough reaches out from the southeastern China, as evident in Fig. 5d. The big ocean monsoon trough is sandwiched between the tropical ridge and subtropical ridge, while the western Pacific subtropical high has retreated to east of Japan. A dry line marks cross-equatorial flow stretching from Borneo to the Celebes Sea. By pentad 42 the convection center is firmly established at 25°N, which resides 10°–15°

farther north than the previous western North Pacific convection zone. Once formed, this oceanic monsoon cyclone is sustained for 40 days.

During its lifetime the monsoon gyre stretches along an east–west axis. At pentad 46 (14–18 August), the gyre reaches its height. An elongated convection zone spreads from the South China Sea to 170°E (at 20°N). This brings the western North Pacific region its second summer rain surge (Wu and Wang 2000).

Figure 5 clearly shows that the western Pacific subtropical high, particularly the western end of ridge, regulates the subseasonal change in East Asia. The subtle shift from the pre-mei-yu to mei-yu front as well as the jump of the rain belt in the western North Pacific are all controlled by the position and movement of the western Pacific subtropical high ridge.

At the Indian subcontinent there looms another component of the second FAC. Over northern India, the rainy season has abided since mid-June. This rain system is a remnant of the northward-moving CISO from the previous monsoon outbreak. Though it starts early, it does not pick up full intensity until the second monsoon outbreak. The climatological rainfall time series of New Delhi (29°N, 77°E), for example, registers the onset date during pentad 35, but the peak rainfall does

CMT Rdg20 1~25(W) 27~39(G) 41~50(R) ptd

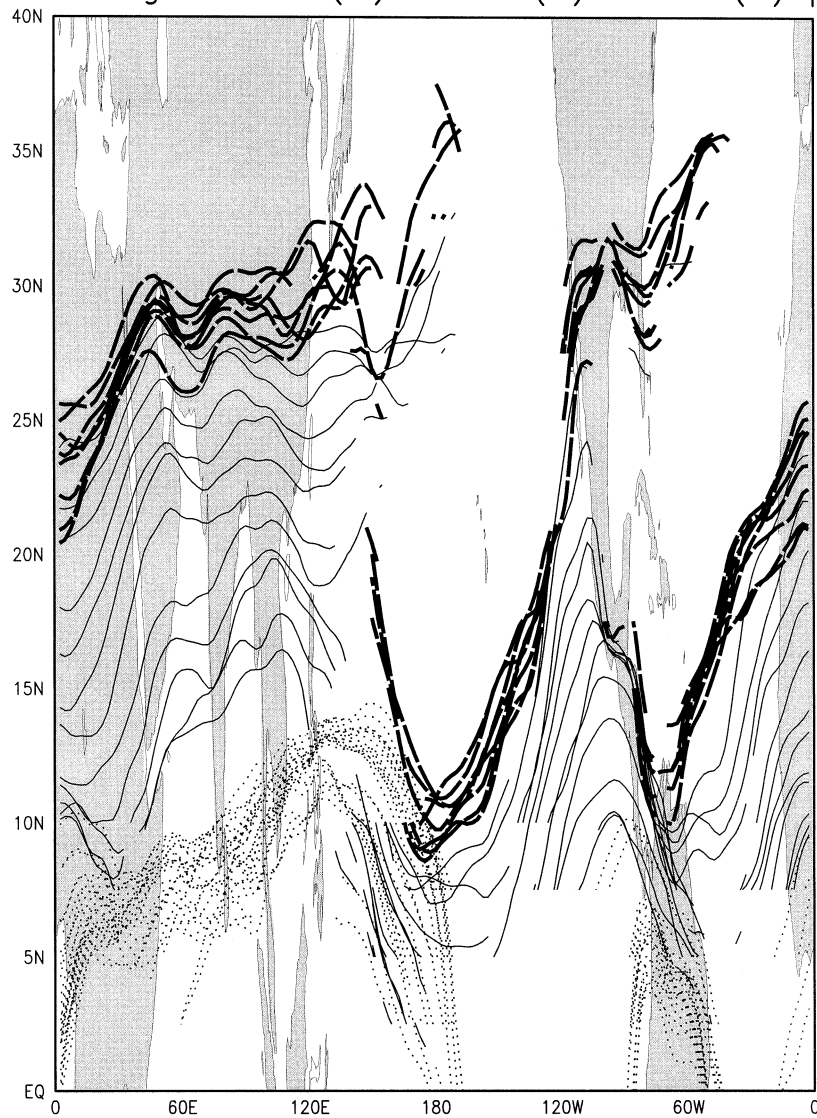


FIG. 9. The annual march of global subtropical ridgelines at 200 hPa. The north–south coordinate has been stretched to highlight the meridional excursion. The lines are grouped into the pre-APSM period (dotted lines, pentads 1–25), the first outbreak cycle (thin lines, pentads 27–39), and the second outbreak cycle (thick-dashed lines, pentads 41–50).

not take place until pentad 42. The lasting rainy season in continental India proves a reverse to the very brisk rainy season just a short distance upstream in the south-east Arabian Sea, where the monsoon rain begins in late May and quickly fades away after three or four weeks (also see monsoon calendar in Fig. 14). It appears that the northward shift of continental Indian rain is closely related to similar action in the western North Pacific. As we show later, this is a manifestation of seasonal migration of major circulation systems over the Northern Hemisphere. Near the end of the second monsoon outbreak (pentad 48–50), the two components merge

into a weak trough, whereas rain patches are seen scattering from Calcutta to the Luzon Strait.

Another way to see the jump of convection in the western North Pacific is to examine the climatological change of typhoon trajectories, since the composition of rain-bearing systems constitutes one of the most prominent features to distinguish the East Asian monsoon and the western North Pacific monsoon. Whereas the rain elements of the western North Pacific monsoon are not exclusively tropical cyclones, it is the tropical cyclones that characterize the jump of rain belt convincingly, just as the frontal trajectory map in Fig. 1 reveals the multiple

OLR Fast Annual Cycle

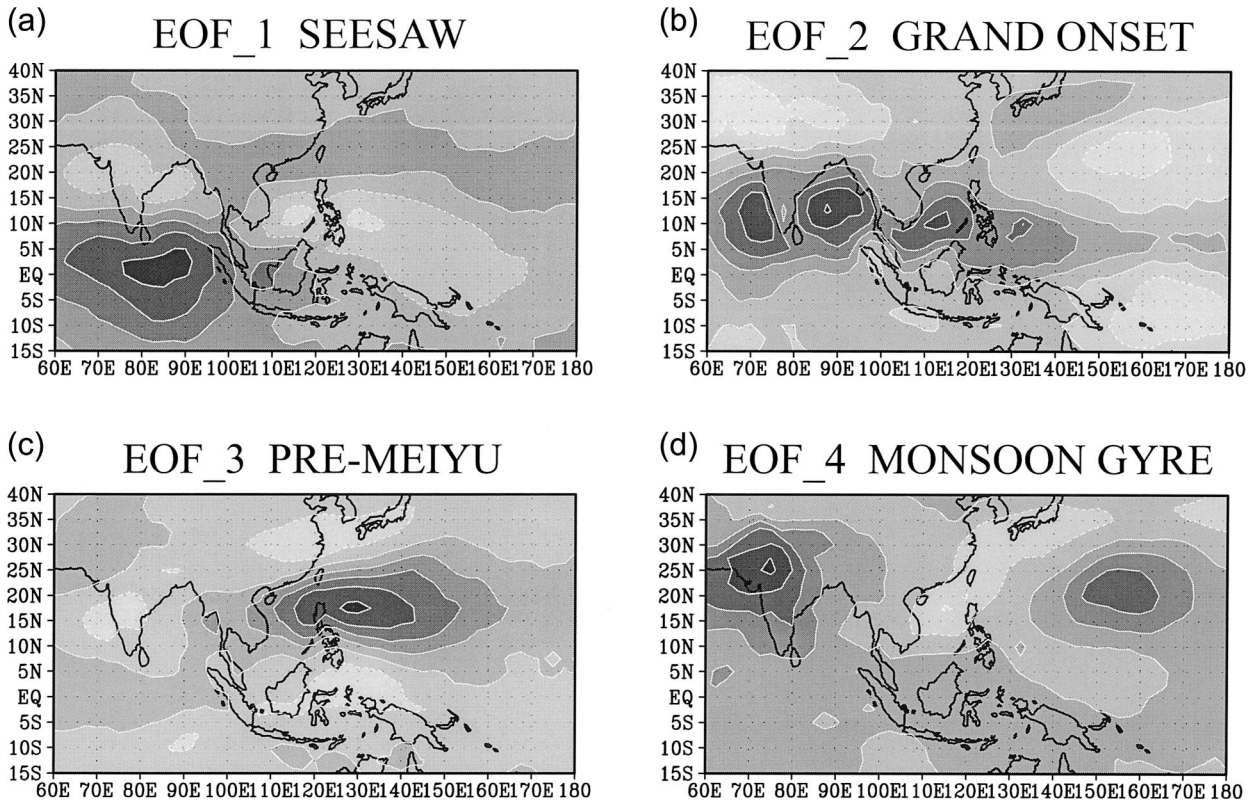


FIG. 10. The four leading EOF modes of the fast annual cycle derived from OLR data: (a) the seesaw mode, (b) the grand-onset mode, (c) the pre-mei-yu mode, and (d) the monsoon gyre mode.

rainy seasons in East Asia. Figure 6 shows sampled 27-yr typhoon trajectories of two periods (pentads 38~39 and 41~42). After subtracting the difference of typhoon occurrences between two neighboring bipentads, Fig. 6c reproduces the rain-belt jump pattern in Fig. 5. It shows that the subseasonal modulation of typhoon occurrence is largely dictated by the APSM FACs.

5. Significance of two monsoon outbreaks

Despite the rather compound subseasonal transition in East Asia, the overall picture of the APSM FAC should be attributed to two major monsoon outbreaks. As Wang and Fan (1999) indicated, the APSM domain can be divided into two subdivisions. The west section ($10^{\circ}\sim 30^{\circ}\text{N}$, $60^{\circ}\sim 120^{\circ}\text{E}$) contains the Indian subcontinent and its adjacent seas. The east section ($10^{\circ}\sim 30^{\circ}\text{N}$, $120^{\circ}\sim 180^{\circ}\text{E}$) contains mainly the western North Pacific. Yet the geographic demarcation could be misleading unless the rain patterns are examined in a time-space frame simultaneously. The local rainy seasons are often multiple and part of a still larger structure, originating from different remote sources. The shape of two monsoon outbreaks can roughly determine the subdivision domain, but only roughly.

Figure 7a shows the square of the FAC CMAP rain, averaged over two subdivisions. It shows that two monsoon outbreaks stand out as the primary forcing of the APSM. The first outbreak peaks during the middle of June (pentads 33~34), while the west section retains the most rain. The second outbreak, a twin peak, occurs near the end of July and the middle of August (pentads 42, 46). The twin peak mainly results from a bimodal distribution of the monsoon gyre onset dates (Ueda and Yasunari 1996). The western North Pacific holds a large part of rain produced by the second monsoon outbreak.

During the first cycle a minor peak also arises in the east section at pentad 30, and another one around pentads 35~38. Those two weak signals in the east section correspond to the pre-mei-yu and mei-yu-lower western North Pacific monsoon, respectively. The second minor peak lagged behind the major peak, that is, the Indian monsoon onset, suggesting a west-to-east migration of convection during the grand-onset event.

The rain intensity of the second outbreak matches quite well the first one. Between two outbreaks stands a brief recess of rain in mid-July. The two outbreaks are easily identified as the peak phases of two FACs. Thus the APSM can be divided in time into the first FAC, from pentad 27 to 38 (from 10 May to 10 July)

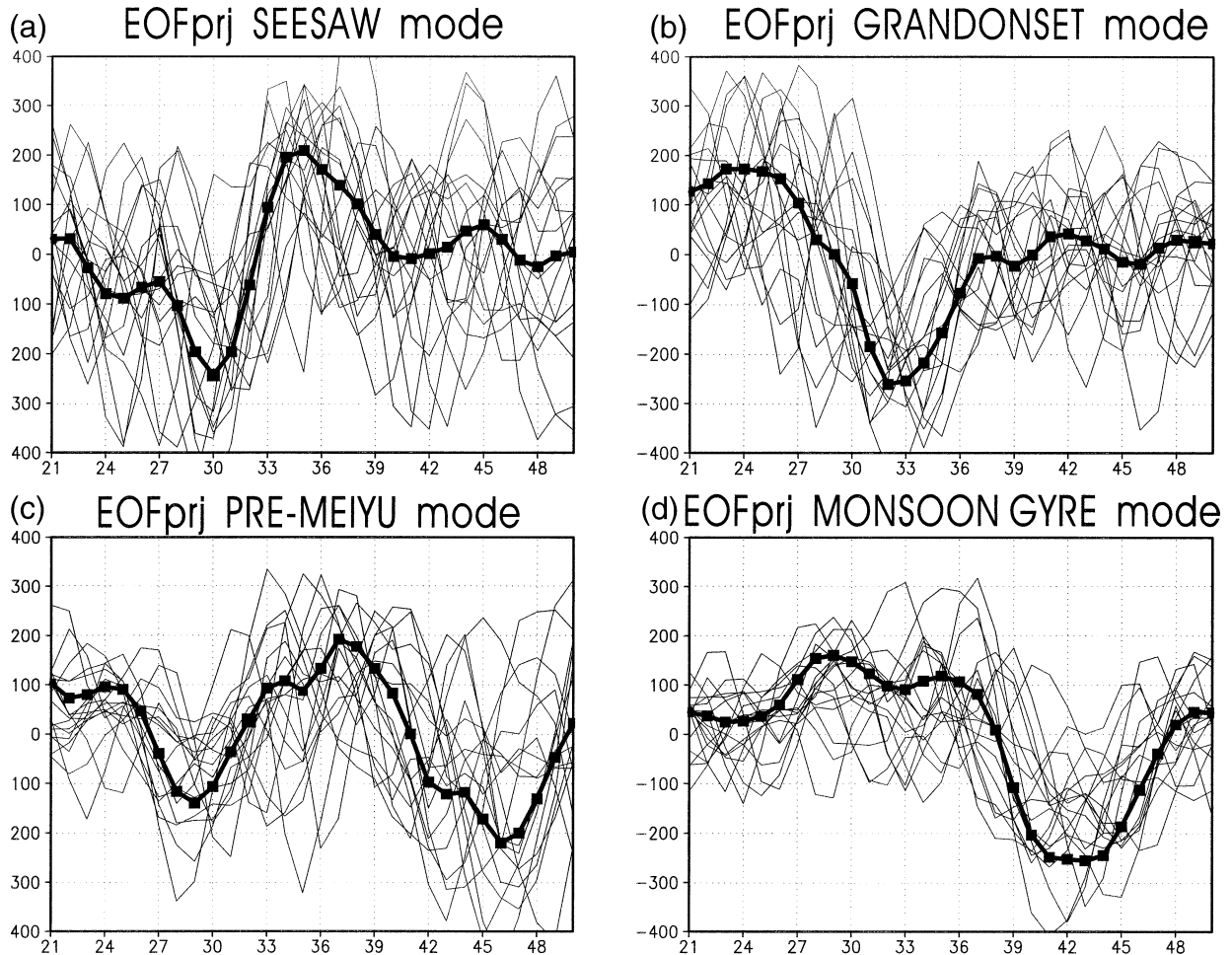


FIG. 11. The projections of the four leading EOF modes [(a)–(d)] upon each of 21 summers (1979–99), are the numerous thin lines. The thick line represents the climatological EOF projection. The recurrent rates appear very high around peak phase, implying a tight phase locking of each EOF mode to the solar calendar.

and the second FAC, from pentad 40 to 51 (from 20 July to 10 September). Each cycle lasts about 50 days.

The vertically integrated diabatic heating rate of NCEP reanalysis data was also calculated (Fig. 7b) according to the method developed by Hoskins et al. (1989). The time–space changes of the diabatic heating agree well with those derived from CMAP data in timing but show discrepancies in magnitude during the second cycle. This asymmetry appears to be caused by a common inability of simulating the western Pacific rain properly in numerical models. A comparison of 14 Atmospheric Model Intercomparison Project (AMIP) GCM runs showed that almost all GCM-simulated monsoon gyres were dislocated and feeble.

A caution is in order at this point with regard to the preceding discussion. Whereas the FACs appear to be a vital fixture of the APSM climatology, they are still dominated by the convection of the slow annual cycle centered at the Bay of Bengal. On the other hand it would be awkward to study the APSM without an FAC

view, as evidenced by the drastic change of bulk rain movement between the two FACs.

In Fig. 8, the statistical CMAP rain movement is measured by the lag correlation in the form of a vector. The direction of the vector points to the surrounding grid with which the lag-1 correlation reaches a maximum value. The length of the vector is proportional to the magnitude of the correlation coefficient. The lag correlation (lagged by one pentad) is computed from the 21-yr CMAP pentad data.

It can be seen that, during the first FAC, the primary rain movements are packed within the Arabian Sea and the Bay of Bengal. The cloud clusters propagate to the east in the tropical region then detour north toward the west coast of India and the head of the Bay of Bengal. The mechanism that governs northward propagation of intraseasonal oscillation convection over the Indian sector is still under debate. Webster (1983) showed that atmosphere–land surface interaction relating to land surface hydrology could induce a northward propagation

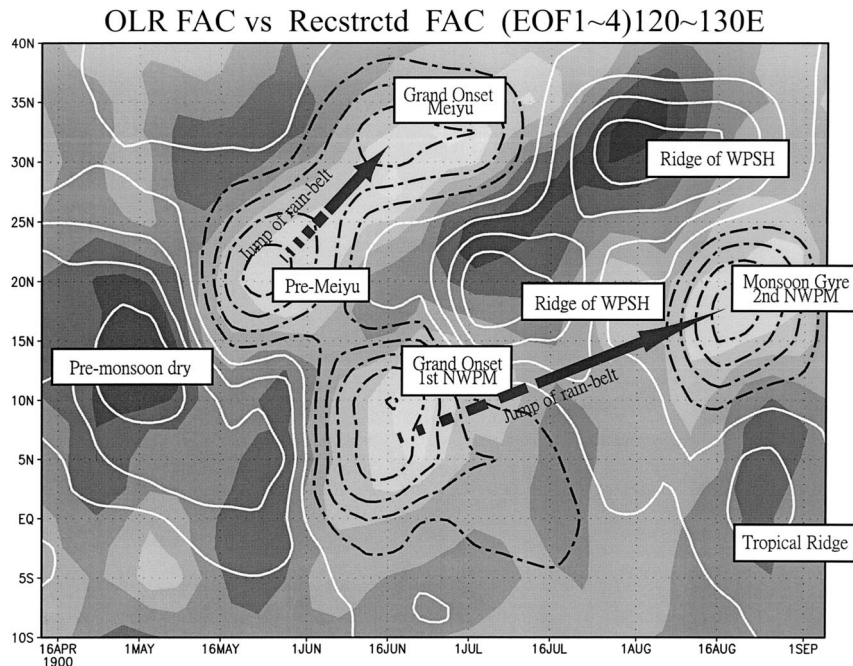


FIG. 12. The Hovmöller diagram of the climatological OLR fast annual cycle along 120°–130°E. The shaded areas denote observations and the contoured areas represent the reconstructed fast annual cycle from the summation of four leading EOF modes. This diagram captures the essentials for the East Asia part of the APSM, which can be confined into a simplified dynamical system with very limited degrees of freedom.

of the intraseasonal oscillation convection over the land, yet his theory failed to explain the prominent northward propagation over the ocean. The meridional monsoon circulation is another candidate that provides a favorable background for northward propagation (Anderson and Stevens 1987). Recently, Kemball-Cook and Wang (2001, hereafter KCW01) have presented evidence showing that air–sea coupling might play a critical role in the northward-propagating intraseasonal oscillation in the Indian Ocean. The essential process is a thermodynamic coupling: enhanced convection cools the ocean beneath and equatorward due to increased cloud cover and evaporation, meanwhile it warms the ocean to its poleward due to opposing processes. The warming to the north then attracts intraseasonal oscillation convection further northward.

During the second FAC, the center of rain activities shifts to the western North Pacific. The rain movement also exhibits a strong westward component. At this time the western Pacific subtropical high has shifted to east of Japan (as shown in Fig. 5d) and the monsoon trough (gyre) intrudes from southeastern China toward the western North Pacific. The westward propagation over the western North Pacific was found on multiple time-scales including 10–20 days, 30–40 days, (Murakami 1984; Chen and Murakami 1988) and about 8–9 days (Lau and Lau 1990). The 8–9-day and biweekly disturbances are primarily convectively coupled equatorial Rossby waves, which often emanate from the equatorial

Pacific near the date line (Nitta 1987) toward the northwest. The emanation could be modulated by the equatorial eastward-propagating Madden–Julian oscillation (MJO) on a 30–40-day timescale; that is, when the equatorial MJO decays over the equatorial central Pacific, the equatorial Kelvin–Rossby wave package disintegrates and releases Rossby waves escaping northwestward (Wang and Xie 1997). These moist equatorial Rossby waves can be strongly enhanced by easterly vertical shears in the monsoon region (Wang and Xie 1996) and possibly enhanced by air–sea interaction (Wang and Xie 1998; KCW01).

6. Two-step boreal summer: A global scenario

Figure 7 demonstrates that the two APSM FACs divide the APSM more or less evenly into two parts, where the division occurs over 20–29 July. We postulate that the abrupt change from the first to the second FAC is really part of a global event, an event attested to by the sudden pause exhibited by the northward shift of major circulation systems in the Northern Hemisphere. During 20–29 July the annual march of climatological upper subtropical ridgelines experiences a major transformation of conduct. Note that the ridgeline is simply the line of $u = 0$, under the condition that local vorticity is negative. The upper ridgeline separates the tropical easterly from the midlatitude westerly regimes. It also marks the position of the upper anticyclone that spans

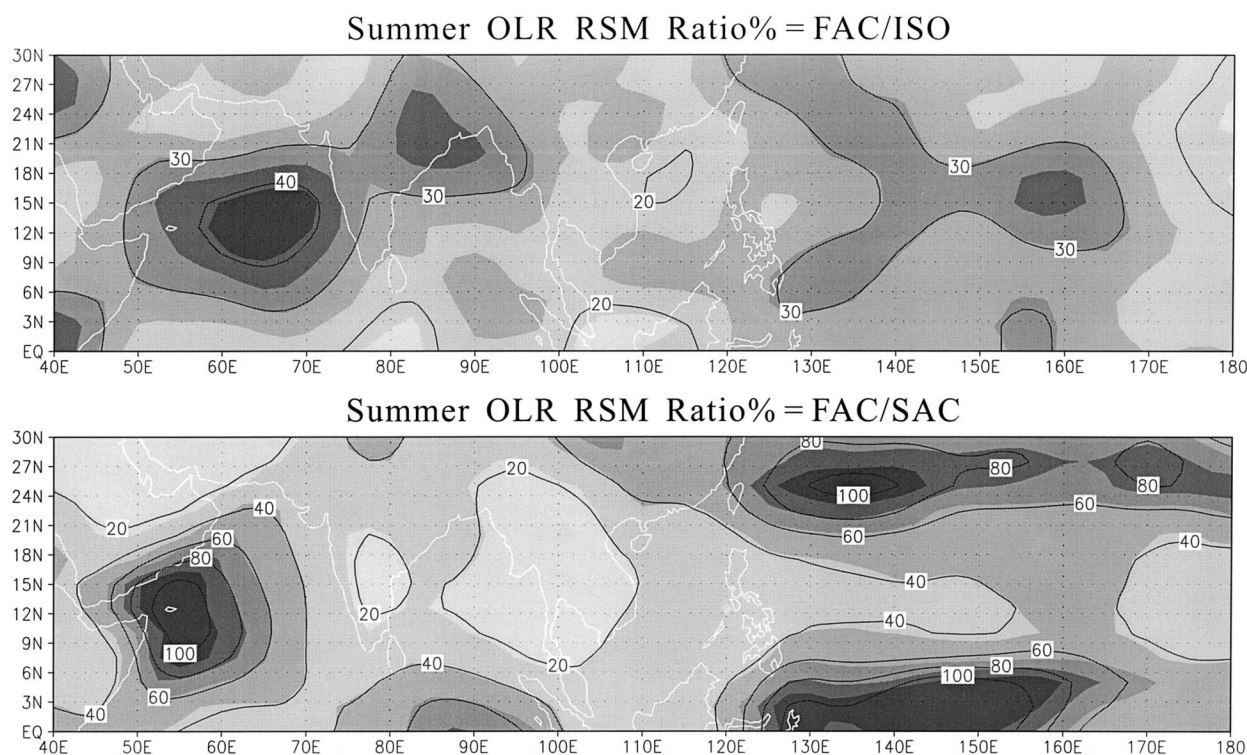


FIG. 13. (lower) The ratio of the OLR rms amplitudes between the fast and slow annual cycles averaged over pentads 25–51 (1979–98); (upper) the ratio of the OLR rms amplitudes between the fast and total intraseasonal variations averaged over the same period.

the outflow generated by monsoon convection; for example, the South Asian high and Mexican high.

The annual march of the subtropical ridgelines at 200 hPa is presented in Fig. 9. It can be seen that, before May, the ridgelines (dotted lines) in the Northern Hemisphere stay in their winter position at south of 12°N. The narrow range of excursion signifies a relatively stable state of the upper high in winter. Only after pentad 27 (11–15 May, see thin lines) do all ridgelines start a long march along the meridional cross section. The northward movement of the ridgeline is swift and global. The size and shape of continents determine the speed and orientation of movement. The movement proceeds until the upper ridges reach their northern limits around pentad 41 (19–24 July). Afterward, during the entire period of the second APSM cycle, the ridgelines (thick lines) are confined to a narrow passageway. This suggests the first FAC should represent a developing stage, and only in the second FAC has the boreal summer matured to the point that the monsoon forcing, seasonal insolation, and global circulation all reach an equilibrium state.

The abrupt change around 20 July results from basin-wide seasonal heating of the Pacific and Atlantic, which also relates to interhemispheric interaction of different monsoon systems. This event is one of the most crucial topics for boreal summer climatology. Its significance needs to be treated in a separated study.

7. A simplified monsoon system as composed by FAC EOF modes

Most APSM characteristics of the FAC can be extracted from the EOF analysis. The EOF analysis was performed on the 21-yr (1979–99) filtered OLR time series over the period from pentad 21 to 50 (11 April–7 September). The grid resolution is $2.5^\circ \times 2.5^\circ$ and the domain is 15°S – 40°N , 60° – 180°E . The results show that it only takes four leading EOF modes (11%, 9%, 8%, 5% of total variance, respectively) to duplicate the major features of the time–space structure of the FAC component of the APSM. The top four EOF patterns are portrayed in Fig. 10. Their projections on individual years, Fig. 11, confirm that all four modes display tight phase locking with the solar calendar. The high recurrence rate from year to year further certifies the existence of the FACs.

The four leading EOF modes will be called the “see-saw” mode, the “grand-onset” mode, the “pre-mei-yu” mode, and the “monsoon gyre” mode. Each EOF mode can be fit into descriptions as follows.

- 1) *The seesaw mode.* This mode (Fig. 10a) has a structure similar to the canonical form of the MJO found by Zhu and Wang (1993). It consists of an east–west dipole with two foci, one over the equatorial Indian Ocean and the other around the Philippine Islands. The equatorial Indian Ocean center is seen in op-

posite phase to a northern counterpart at the Indian subcontinent, a much weaker fraction. Nevertheless, this north–south dipole suggests the northward advancement of rain before the Indian monsoon onset. As Fig. 11a exhibits, the seesaw mode shows some precursory signs before pentad 27, and becomes very active from pentad 28 to pentad 38 during the first cycle. Around pentad 33, the onset time of the Indian monsoon, the seesaw mode goes through a rapid phase change, suggesting that the tropical Indian Ocean rain moves north and east, a well-known behavior of the summer intraseasonal oscillation (Lau and Chan 1986).

- 2) *The grand-onset mode.* This mode (Fig. 10b) takes its name from Wang and Xu (1997). It has been described fully in section 4. Here we only note that the grand-onset mode has been built up from a rapid sequence of local onsets. The onset events take place at the Arabian Sea (15° – 20° N, 62.5° – 67.5° E), the Bay of Bengal (pentad 32, 15° – 20° N, 90° – 95° E), the South China Sea (pentad 33, 7.5° – 12.5° N, 115° – 120° E) and the lower western North Pacific (pentad 34, 7.5° – 12.5° N, 130° – 135° E). This series of onsets happens almost simultaneously, implying a type of linear instability of the monsoon trough (Krishnakumar and Lau 1997).
- 3) *The pre-mei-yu mode.* The isolation of this mode (Fig. 10c) reconfirmed that the brief pre-mei-yu period is indeed an independent event. However, it also amplifies during the second FAC. The reason is simple since this mode develops whenever the western Pacific subtropical high loses ground. It dominates for three weeks around pentad 28; afterward, the western Pacific subtropical high ridge does a second retreat. Then the same pattern emerges again near the end of the boreal summer (pentad 46). When the western North Pacific monsoon prospers, it will signal another retreat of the subtropical high.
- 4) *The monsoon gyre mode.* The name (Fig. 10d) was drawn from the typhoon community. Nevertheless this mode is composed of two components—a monsoon gyre over the western North Pacific and another convection center close to the southern foot of the Himalayas. It appears solely in the second half of summer.

The reconstructed FACs based on the four leading EOF modes mimic many monsoon features, particularly those in the East Asia sector, as shown in Fig. 12. Figure 12 recaptures the rain-belt jump from the South China Sea to the Yangtze River, and the multiple rainy seasons over the western North Pacific. The reconstructed time series has succeeded in reproducing the advance/retreat of the western Pacific subtropical high ridge. It is remarkable that many subtle details in East Asia can be reproduced by this simple system with only *four* components. The structure of the EOF modes indicates that the FACs are inversely linked by the phase of dry and

rainy areas. The dry area often indicates where a rainy area would emerge next. The evolution from the seesaw to grand onset, and further to the monsoon gyre, apparently follows the same pattern.

8. Summary: A monsoon calendar

In this study we propose to treat the phase-locked intraseasonal variations of the APSM as part of an annual cycle. Thus the time–space structure of the APSM is bound to a fine-resolution climatology. A monsoon calendar can be designed in pentad resolution; nevertheless its domain covers the whole Asian–Pacific summer monsoon area. The boreal summer was recognized as comprising two periods, each containing a major monsoon outbreak. The two periods are divided in late July by an abrupt change of global proportions.

To complete this picture we need to recognize the relative importance between the slow- and fast-varying part of annual cycle, and the relative percentage of the fast annual cycles to the total intraseasonal variability, since the APSM is also known for its strong interannual variability on intraseasonal timescales (e.g., Sperber et al. 2000; in their study the daily climatological average at each grid has already been removed). To do so we calculated the rms amplitudes of the OLR slow and fast annual cycles from pentad 25 to pentad 51, and the total rms amplitudes of intraseasonal oscillations within the same period from 1979 to 1998. The ratio of FAC to SAC (lower panel in Fig. 13) reveals that the SAC dominates in the Bay of Bengal and entire Indochina Peninsula, as expected. In the Arabian Sea the SAC and FAC are about equal, yet the FAC has an edge over the SAC along the mei-yu (25° N) and north of New Guinea (5° N). As for the ratio between the fast annual cycle and total intraseasonal oscillation, the climatological component comes out strong in the Arabian Sea, registering 45% around 14° N, 65° E, and the northeastern corner of India (lower panel of Fig. 13). The FAC also has a powerful presence in the western North Pacific. The FAC is weak in the Indochina Peninsula and upper South China Sea. The strong phase-locking of oceanic convection to the solar calendar along 15° N manifests again the timely northward shift of the major circulation pattern in late July. Overall, we should be reminded that to define the FAC precisely from a climatological time series is a rather stringent way to quantify the APSM singularities. It has the advantage of testing statistical significance rigorously; for example, Wang and Xu (1997). However, the local experiences of the monsoon subseason were extracted from events in a well-ordered sequence. The variation in time is expected and tolerated. In many cases, a composite study appears to be a better alternative to examine the subseason's features.

Finally, an APSM calendar (Fig. 14a) was designed to summarize this study. For various key locations (see map in Fig. 14b) we have inscribed the onset, peak, and length of rainy seasons that characterize the local fast

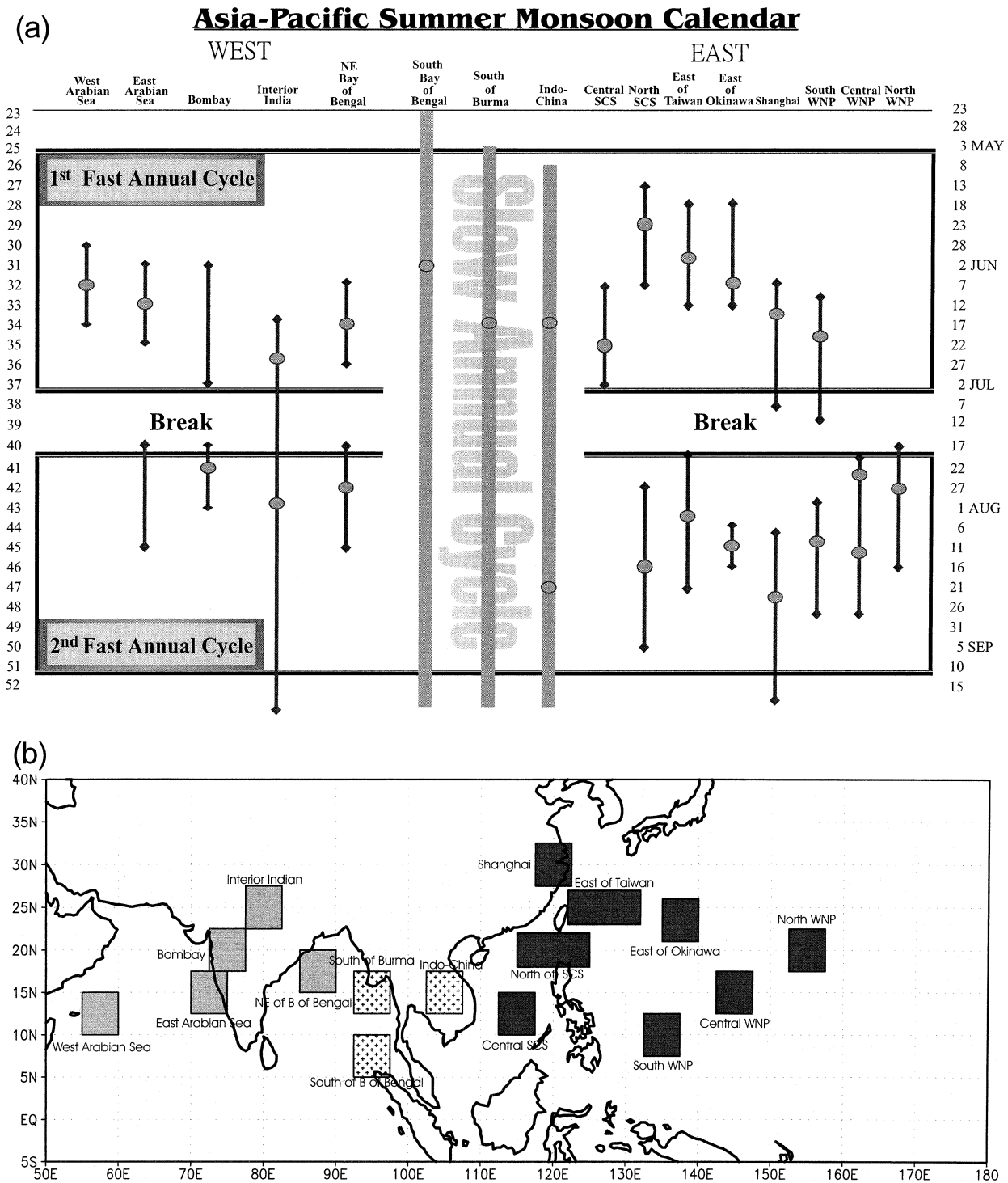


FIG. 14. The monsoon calendar of the APSM at various key locations. (a) The onset, peak, and withdraw dates at each spot; and the length of rainy season. Many areas undergo multiple rainy seasons or exhibit double peaks. The arrows show the length of fast annual cycle—the period with intense, lasting rainfall in local area. The ovals mark the pentad when rainfall reaches a peak. The locations near the Indochina Peninsula are dominated by the slow annual cycle. (b) A map of the locations.

annual cycles. In several locations it is the slow annual cycles that predominated. Note that most areas experience multiple rainy seasons.

It remains to be seen how well the FACs can be simulated in numerical experiments; for instance the AMIP project (Gates 1992). A preliminary study of 12 AMIP-2 runs reveals some consistent outcomes. To begin with, all performed reasonably well on the timing of the Indian monsoon onset. All did poorly to simulate mei-yu. Only a few managed to reproduce the WMP monsoon at the peak of the grand-onset. All showed a rapid decline of model performance during the second FAC. All models encountered difficulties in simulating the monsoon gyre, which appeared either too early or misplaced to the east; for some models the monsoon gyre did not show up at all. Finally, a common discrepancy is that the subsidence area did not display a sharp definition as observed. To be more specific, the agile movement of the western Pacific subtropical high ridge was not captured by most models. A detailed AMIP analysis of the APSM FAC is currently underway.

Acknowledgments. Prof. LinHo is supported by NSC 89-2111-M-002-006-AP7. Dr. Bin Wang is supported by a grant from NOAA Office of Global Change and the ONR Marine Meteorology Program (N00014-96-1-0796). The International Pacific Research Center is sponsored in part by the Frontier Research System for Global Change.

REFERENCES

- Ananthakrishnan, R., and M. K. Soman, 1988: The onset of the Southwest Monsoon over Kerala: 1901–1980. *J. Climatol.*, **8**, 283–296.
- Anderson, J. R., and D. E. Stevens, 1987: The presence of linear wavelike modes in a zonally symmetric model of the tropical atmosphere. *J. Atmos. Sci.*, **44**, 2115–2127.
- Chen, T.-J. G., and C.-P. Chang, 1980: The structure and vorticity budget of an early summer monsoon trough (Mei-Yu) over southeastern China and Japan. *Mon. Wea. Rev.*, **108**, 942–953.
- Chen, T.-C., and M. Murakami, 1988: The 30–40 day variation of convective activity over the western Pacific Ocean with emphasis on the northwestern region. *Mon. Wea. Rev.*, **116**, 892–906.
- , and M. C. Yen, 1991: Interaction between intraseasonal oscillations of the midlatitude flow and tropical convection during 1979 northern summer: The Pacific Ocean. *J. Climate*, **4**, 653–671.
- Ding, Y., 1994: *Monsoons over China*. Vol. 16, *Atmospheric Sciences Library*, Kluwer Academic, 419 pp.
- Gates, W. L., 1992: AMIP: The Atmospheric Model Intercomparison Project. *Bull. Amer. Meteor. Soc.*, **73**, 958–962.
- He, H., J. W. McGinnis, Z. Song, and M. Yanai, 1987: Onset of the Asian summer monsoon in 1979 and the effect of the Tibetan Plateau. *Mon. Wea. Rev.*, **115**, 1966–1995.
- Hoskins, B. J., H.-H. Hsu, I. N. James, M. Masutani, P. D. Sardeshmukh, and G. H. White, 1989: Diagnostics of the global atmospheric circulation based on ECMWF analysis 1979–1989. WMO Tech. Doc. WMO/TD-326, 217 pp.
- Kalnay, E., and Coauthors, 1996: The NCEP/NCAR 40-Year Reanalysis Project. *Bull. Amer. Meteor. Soc.*, **77**, 437–471.
- Kang, I.-S., S.-I. An, C.-H. Joong, S.-C. Yoon, and S.-M. Lee, 1989: 30–60 day oscillation appearing in climatological variation of outgoing longwave radiation around East Asia during summer. *J. Korean Meteor. Soc.*, **25**, 221–232.
- , C.-H. Ho, Y.-K. Lim, and K.-M. Lau, 1999: Principle modes of climatological seasonal and intraseasonal variations of the Asian summer monsoon. *Mon. Wea. Rev.*, **127**, 322–340.
- Kato, K., 1985: On the abrupt change in the structure of the Baiu front over the China Continent in late May of 1979. *J. Meteor. Soc. Japan*, **63**, 737–750.
- Kawamura, R., and T. Murakami, 1998: Baiu near Japan and its relation to summer monsoon over Southeast Asia and the western North Pacific. *J. Meteor. Soc. Japan*, **76**, 619–638.
- Kemball-Cook, S., and B. Wang, 2001: Equatorial waves and air–sea interaction in the boreal summer intraseasonal oscillation. *J. Climate*, **14**, 2923–2942.
- Krishnakumar, V., and K.-M. Lau, 1997: Symmetric instability of monsoon flows. *Tellus*, **49A**, 228–245.
- Krishnamurti, T. N., and H. N. Bhalme, 1976: Oscillation of a monsoon system. Part I: Observational aspects. *J. Atmos. Sci.*, **33**, 1937–1954.
- Lanzante, J. R., 1983: Some singularities and irregularities in the seasonal progression of the 700 mb height field. *J. Climate Appl. Meteor.*, **22**, 967–982.
- Lau, K.-M., and P. H. Chan, 1986: Aspects for the 40–50 day oscillation during the northern summer as inferred from outgoing longwave radiation. *Mon. Wea. Rev.*, **114**, 1354–1367.
- , and N.-C. Lau, 1990: Observed structure and propagation characteristics of tropical summertime synoptic scale disturbances. *Mon. Wea. Rev.*, **118**, 1888–1913.
- , G. J. Yang, and S. H. Shen, 1988: Seasonal and intraseasonal climatology of summer monsoon rainfall over East China. *Mon. Wea. Rev.*, **116**, 18–37.
- Leathers, D. J., and D. A. Robinson, 1997: Abrupt changes in the seasonal cycle of North American snow cover. *J. Climate*, **10**, 2569–2585.
- Lu, M.-M., and Y. L. Chen, 2001: Large-scale features associated with the extremely early and late onset of the South China Sea summer monsoon. *Terr. Atmos. Oceanic Sci.*, in press.
- Matsumoto, J., 1992: The seasonal changes in Asian and Australian monsoon regions. *J. Meteor. Soc. Japan*, **70**, 257–273.
- Murakami, M., 1984: Analysis of the deep convective activity over the western Pacific and Southeast Asia. 2. Seasonal and intraseasonal variation during northern summer. *J. Meteor. Soc. Japan*, **62**, 88–108.
- Nakazawa, T., 1992: Seasonal phase lock of intraseasonal variation during the Asian summer monsoon. *J. Meteor. Soc. Japan*, **70**, 597–611.
- Ninomiya, K., and H. Muraki, 1986: Large-scale circulation over East Asia during Baiu period 1979. *J. Meteor. Soc. Japan*, **64**, 409–429.
- Nitta, T., 1987: Convective activities in the tropical western Pacific and their impact on the Northern Hemisphere summer monsoon. *J. Meteor. Soc. Japan*, **65**, 373–390.
- Sadler, J. C., 1976: A role of the tropical upper tropospheric trough in early season typhoon development. *Mon. Wea. Rev.*, **104**, 1266–1278.
- Sperber, K. R., J. M. Slingo, and H. Annamali, 2000: Predictability and the relationship between subseasonal and interannual variability during the Asian summer monsoon. *Quart. J. Roy. Meteor. Soc.*, **126**, 2545–2574.
- Tao, S., and L. Chen, 1987: A review of recent research on the East Asian summer monsoon in China. *Monsoon Meteorology*, C.-P. Chang and T. N. Krishnamurti, Eds., Oxford University Press, 60–92.
- Tanaka, M., 1992: Intraseasonal oscillation and the onset and retreat dates of the summer monsoon over east, southeast Asia and the western Pacific region using GMS high cloud amount data. *J. Meteor. Soc. Japan*, **70**, 613–629.
- Ueda, H., and T. Yasunari, 1996: Maturing process of the summer

- monsoon over the western North Pacific—A coupled ocean/atmosphere system. *J. Meteor. Soc. Japan*, **74**, 493–508.
- , —, and R. Kawamura, 1995: Abrupt seasonal change of large-scale convection activity over the western Pacific in northern summer. *J. Meteor. Soc. Japan*, **73**, 795–809.
- Wang, B., and X. Xie, 1996: Low-frequency equatorial waves in vertically sheared zonal flow. Part I: Stable waves. *J. Atmos. Sci.*, **53**, 449–467.
- , and —, 1997: A model for the boreal summer intraseasonal oscillation. *J. Atmos. Sci.*, **54**, 72–86.
- , and X. Xu, 1997: Northern Hemisphere summer monsoon singularities and climatological intraseasonal oscillation. *J. Climate*, **10**, 1071–1084.
- , and Z. Fan, 1999: Choice of South Asia summer monsoon indices. *Bull. Amer. Meteor. Soc.*, **80**, 629–638.
- Webster, P. J., 1983: Mechanisms of monsoon low-frequency variability: Surface hydrological effects. *J. Atmos. Sci.*, **40**, 2110–2124.
- , 1996: Intraseasonal variability of the coupled monsoon system and its relationship to predictability of climate. Preprints, *Int. Workshop on the Climate System of Monsoon Asia*, Kyoto, Japan, Meteor. Soc. Japan, 14–17.
- Wu, R., and B. Wang, 2000: Multi-stage onset of summer monsoon over the western North Pacific. *Climate Dyn.*, **17**, 277–289.
- Xie, P., and P. A. Arkin, 1997: Global precipitation: A 17-year monthly analysis based on gauge observations, satellite estimates and numerical model outputs. *Bull. Amer. Meteor. Soc.*, **78**, 2539–2558.
- Yanai, M., C. Li, and Z. Song, 1992: Seasonal heating of the Tibetan Plateau and its effects on the evolution of the Asian summer monsoon. *J. Meteor. Soc. Japan*, **70**, 319–351.
- Yoshino, M. M., 1965: Four stages of the rainy season in early summer over East Asia (Part I). *J. Meteor. Soc. Japan*, **43**, 231–245.
- Zhu, B., and B. Wang, 1993: The 30–60 day convection seesaw between the tropical Indian and western Pacific Oceans. *J. Atmos. Sci.*, **50**, 184–199.